JOC Article
pubs.acs.org/joc

A Mechanistic Investigation into the Zinc Carbenoid-Mediated Homologation Reaction by DFT Methods: Is a Classical Donor−Acceptor Cyclopropane Intermediate Involved?

Wilhelm A. Eger, Charles K. Zercher,[‡] and Craig M. Williams*[,†]

[†]*School of Chemistry and Molecular Bioscience, University of Queensland, St. Lucia, Brisbane, QLD 4067, Australia, and* [‡]*Department of Chemistry, University of New Hampshire, Durham, New Hampshire 03824*

c.williams3@uq.edu.au

Received August 13, 2010

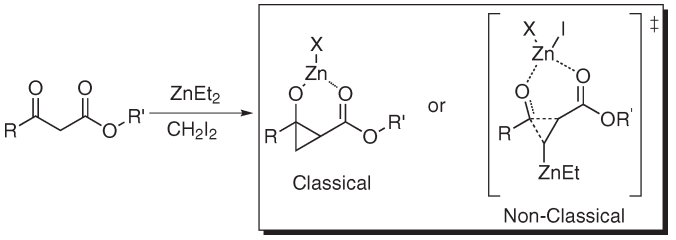

An extensive density functional theory (DFT, M05-2X) investigation has been performed on the zinc carbenoid-mediated homologation reaction of β-keto esters. The mechanistic existence of a classical donor−acceptor cyclopropane intermediate was probed to test the traditional school of thought regarding these systems. Calculations of the carbenoid insertion step, following enolate formation, unmasked two possible pathways. Pathway B was shown to explain the proposed, but spectroscopically unobservable donor−acceptor cyclopropane intermediate, while the second (pathway A) reveals an alternative to the classical intermediate in that a cyclopropane *transition state* leads to product.

Introduction

One carbon homologation (unitary chain extension) is a valued transformative synthetic tool for the efficient creation of molecular structure. Generally, however, such methods, for example, the Arndt-Eistert reaction[1] (via Wolff rearrangement[2]) or the Wittig reaction ($MeOCHPPh_3$),[3] are both somewhat dated and can carry unwanted functional groups requiring further manipulation for their removal. Over the past decade Zercher et al. have described efforts in developing CH_2 homologation to construct in a one-step/one-pot system syntheses of γ-keto esters (see Scheme 1) from β-keto esters (**I**), using Furukawa's reagent ($EtZnCH_2I$)[4] (see Scheme 1).[5]

Application of this powerful methodology has found utility in the construction of complex ring systems.[6] Additional investigations have expanded the field of substrates to include β-keto phosphonates[7] and amides.[8] Substantial variation of this reaction is possible through the application of tandem reaction processes, for example, the introduction of residues at the α-position (such as hydroxyalkyl,[9] alkyl,[8] and iodomethyl[10]) or at the β-position with modified alkyl carbenoids.[11] Although this mild and efficient reaction functions superbly with simple systems, some substrates that include isolated double bond functionality[5] and cyclic or α-substituted β-keto ester derivatives react poorly, which results in significantly decreased yields.[12]

In addition to the mildness of the conditions, the one-step methodology offers additional advantages compared to

(1) Fuchter, M. J. *Name React. Homol.* **2009**, 336.
(2) Kirmse, W. *Eur. J. Org. Chem.* **2002**, *2002*, 2193.
(3) Galatsis, P. *Name React. Homol.* **2009**, 588.
(4) (a) Furukawa, J.; Kawabata, N.; Nishimura, J. *Tetrahedron Lett.* **1966**, *7*, 3353. (b) Furukawa, J.; Kawabata, N.; Nishimura, J. *Tetrahedron* **1968**, *24*, 53. (c) Lehnert, E. K.; Scott Sawyer, J.; Macdonald, T. L. *Tetrahedron Lett.* **1989**, *30*, 5215. (d) Charette, A. B.; Marcoux, J.-F. *J. Am. Chem. Soc.* **1996**, *118*, 4539.
(5) Brogan, J. B.; Zercher, C. K. *J. Org. Chem.* **1997**, *62*, 6444.
(6) (a) Heim, R.; Wiedemann, S.; Williams, C. M.; Bernhardt, P. V. *Org. Lett.* **2005**, *7*, 1327. (b) Tilly, D. P.; Williams, C. M.; Bernhardt, P. V. *Org. Lett.* **2005**, *7*, 5155. (c) Schwartz, B. D.; Tilly, D. P.; Heim, R.; Wiedemann, S.; Williams, C. M.; Bernhardt, P. V. *Eur. J. Org. Chem.* **2006**, *2006*, 3181.
(7) Verbicky, C. A.; Zercher, C. K. *J. Org. Chem.* **2000**, *65*, 5615.
(8) Hilgenkamp, R.; Zercher, C. K. *Tetrahedron* **2001**, *57*, 8793.
(9) Lai, S.; Zercher, C. K.; Jasinski, J. P.; Reid, S. N.; Staples, R. J. *Org. Lett.* **2001**, *3*, 4169.
(10) Pu, Q.; Wilson, E.; Zercher, C. K. *Tetrahedron* **2008**, *64*, 8045.
(11) (a) Furukawa, J.; Kawabata, N.; Nishimura, J. *Tetrahedron Lett.* **1968**, *9*, 3495. (b) Lin, W.; McGinness, R. J.; Wilson, E. C.; Zercher, C. K. *Synthesis* **2007**, *2007*, 2404.
(12) Ronsheim, M. D.; Zercher, C. K. *J. Org. Chem.* **2003**, *68*, 1878.

Published on Web 09/29/2010 DOI: 10.1021/jo101590t

SCHEME 1. Proposed Mechanism of the Zinc Carbenoid-Mediated Chain Extension Reaction Based upon Classical Donor−Acceptor Cyclopropane Cleavage

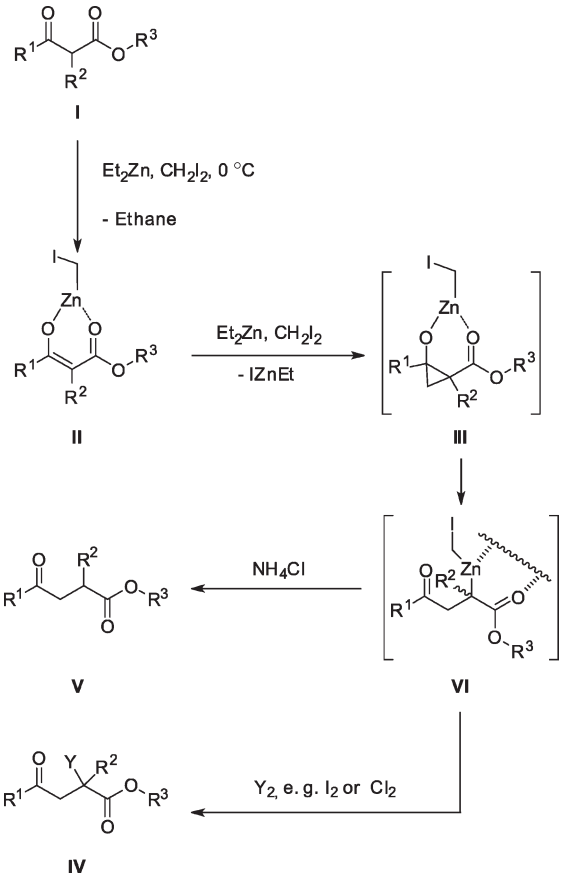

related syntheses of γ-keto esters.[13,14] For example, the creation of the initial enolate ion does not require an additional step, as the Furukawa reagent is able to fulfill this requirement. Additionally, the zinc carbenoid-mediated reaction functions with β-keto ester starting materials that are unsubstituted at the α-position and, therefore, outcompetes the radical variant,[14] although the Saigo method includes some examples of unsubstituted dicarbonyls.[13h,i]

The proposed mechanistic intermediate for related methods (i.e., cyclopropanation of enol ethers[13d,k]) is a donor−acceptor cyclopropane,[15] which undergoes fragmentation resulting in one carbon homologation.[13b,e−h,j] Upon first analysis the zinc carbenoid-mediated reaction developed by Zercher is no different in that a cyclopropane intermediate can also be proposed to effect transformation (Scheme 2).[14] However, extensive spectroscopic analysis by Zercher[7] failed to reveal any evidence of such an intermediate, which is contrary to observable spectroscopic evidence of cyclopropane intermediates for the Simmons−Smith reaction.[13a,c,i,16a,b] Accordingly, an alternate mechanism that does not include a cyclopropane intermediate may be operable.

As the ethyl(iodomethyl)zinc reagent is similar to the copper-activated iodo(iodomethyl)zinc compound used in the Simmons−Smith reaction, it is conceivable that these reactions may follow the same or similar mechanisms. There are several detailed computational studies that have investigated the mechanism of the Simmons−Smith reaction,[17] but most of these used chlorine atoms (even though some key intermediates and transition states of the Simmons−Smith reaction have been calculated with iodine,[17j,12] the whole reaction sequence has never been investigated), which avoids extensive computational time associated with studying iodine atoms. Although chlorine-containing Simmons−Smith reagents, and in particular $EtZnCH_2Cl$, have been reported to be superior in reactivity compared to their iodo counterparts,[18] the zinc carbenoid-mediated chain extension reaction is not more efficient when using $EtZnCH_2Cl$.

In this paper we present the results of a detailed DFT[19] study of the zinc carbenoid-mediated chain extension reaction focusing on the one-carbon chain extension of methyl acetoacetate using the Furukawa ($EtZnCH_2I$) carbenoid.[4d] To our knowledge, this reaction has not been the topic of computational analysis and, therefore, it is our aim to provide insights into mechanistic aspects and reaction pathways concentrating on the existence of a donor−acceptor intermediate, i.e., is the classical understanding correct?

Computational Method

All calculations were performed with the program package Gaussian03, Rev. E.01[20] The functional used to obtain the

(13) (a) Simmons, H. E.; Smith, R. D. *J. Am. Chem. Soc.* **1958**, *80*, 5323. (b) Wenkert, E.; McPherson, C. A.; Sanchez, E. L.; Webb, R. L. *Synth. Commun.* **1973**, *3*, 255. (c) Bieraugel, H.; Akkerman, J. M.; Armande, J. C. L.; Pandit, U. K. *Tetrahedron Lett.* **1974**, 2817. (d) Nagata, W.; Yoshioka, M. *Org. React.* (*N.Y.*) **1977**, *25*, 255. (e) Reichelt, I.; Reissig, H. U. *Chem. Ber.* **1983**, *116*, 3895. (f) Kunkel, E.; Reichelt, I.; Reissig, H. U. *Liebigs Ann. Chem.* **1984**, 512. (g) Reichelt, I.; Reissig, H. U. *Liebigs Ann. Chem.* **1984**, 531. (h) Saigo, K.; Kurihara, H.; Miura, H.; Hongu, A.; Kubota, N.; Nohira, H.; Hasegawa, M. *Synth. Commun.* **1984**, *14*, 787. (i) Saigo, K.; Yamashita, T.; Hongu, A.; Hasegawa, M. *Synth. Commun.* **1985**, *15*, 715. (j) Reissig, H. U. *Top. Curr. Chem.* **1988**, *144*, 73. (k) Miyakoshi, T. *Org. Prep. Proced. Int.* **1989**, *21*, 659.

(14) (a) Dowd, P.; Choi, S. C. *J. Am. Chem. Soc.* **1987**, *109*, 6548. (b) Dowd, P.; Choi, S. C. *J. Am. Chem. Soc.* **1987**, *109*, 3493. (c) Dowd, P.; Choi, S. C. *Tetrahedron Lett.* **1989**, *30*, 6129. (d) Dowd, P.; Choi, S. C. *Tetrahedron* **1989**, *45*, 77.

(15) Reissig, H.-U.; Zimmer, R. *Chem. Rev.* **2003**, *103*, 1151.

(16) (a) Zercher, C. K. Private communication. (b) Orsini, F.; Pelizzoni, F.; Ricca, G. *Tetrahedron Lett.* **1982**, *23*, 3945.

(17) (a) Hida, M. *Bull. Chem. Soc. Jpn.* **1967**, *40*, 2497. (b) Dargel, T. K.; Koch, W. *J. Chem. Soc., Perkin Trans. 2* **1996**, 877. (c) Bernardi, F.; Bottoni, A.; Miscione, G. P. *J. Am. Chem. Soc.* **1997**, *119*, 12300. (d) Hirai, A.; Nakamura, M.; Nakamura, E. *Chem. Lett.* **1998**, 927. (e) Nakamura, E.; Hirai, A.; Nakamura, M. *J. Am. Chem. Soc.* **1998**, *120*, 5844. (f) Hermann, H.; Lohrenz, J. C. W.; Kuhn, A.; Boche, G. *Tetrahedron* **2000**, *56*, 4109. (g) Fang, W.-H.; Phillips, D. L.; Wang, D.; Li, Y.-L. *J. Org. Chem.* **2002**, *67*, 154. (h) Wang, D.; Phillips, D. L.; Fang, W.-H. *Organometallics* **2002**, *21*, 5901. (i) Mori, S.; Nakamura, E. *Yuki Gosei Kagaku Kyokaishi* **2003**, *61*, 144. (j) Nakamura, M.; Hirai, A.; Nakamura, E. *J. Am. Chem. Soc.* **2003**, *125*, 2341.

(18) (a) Denmark, S. E.; Edwards, J. P. *J. Org. Chem.* **1991**, *56*, 6974. (b) Charette, A. B.; Lacasse, M.-C. *Org. Lett.* **2002**, *4*, 3351.

(19) Parr, R. G.; Yang, W. *Density-Functional Theory of Atoms and Molecules*; Oxford University Press: New York, 1989.

(20) Frisch, M. J.; Trucks, G. W.; Schlegel, H. B.; Scuseria, G. E.; Robb, M. A.; Cheeseman, J. R.; Montgomery, J. A., Jr.; Vreven, T.; Kudin, K. N.; Burant, J. C.; Millam, J. M.; Iyengar, S. S.; Tomasi, J.; Barone, V.; Mennucci, B.; Cossi, M.; Scalmani, G.; Rega, N.; Petersson, G. A.; Nakatsuji, H.; Hada, M.; Ehara, M.; Toyota, K.; Fukuda, R.; Hasegawa, J.; Ishida, M.; Nakajima, T.; Honda, Y.; Kitao, O.; Nakai, H.; Klene, M.; Li, X.; Knox, J. E.; Hratchian, H. P.; Cross, J. B.; Bakken, V.; Adamo, C.; Jaramillo, J.; Gomperts, R.; Stratmann, R. E.; Yazyev, O.; Austin, A. J.; Cammi, R.; Pomelli, C.; Ochterski, J. W.; Ayala, P. Y.; Morokuma, K.; Voth, G. A.; Salvador, P.; Dannenberg, J. J.; Zakrzewski, V. G.; Dapprich, S.; Daniels, A. D.; Strain, M. C.; Farkas, O.; Malick, D. K.; Rabuck, A. D.; Raghavachari, K.; Foresman, J. B.; Ortiz, J. V.; Cui, Q.; Baboul, A. G.; Clifford, S.; Cioslowski, J.; Stefanov, B. B.; Liu, G.; Liashenko, A.; Piskorz, P.; Komaromi, I.; Martin, R. L.; Fox, D. J.; Keith, T.; Al-Laham, M. A.; Peng, C. Y.; Nanayakkara, A.; Challacombe, M.; Gill, P. M. W.; Johnson, B.; Chen, W.; Wong, M. W.; Gonzalez, C.; Pople, J. A. *Gaussian03*, Rev. E.01; Gaussian Inc., Wallingford, CT, **2004**.

SCHEME 2. Mechanism of the Deprotonation Step[a]

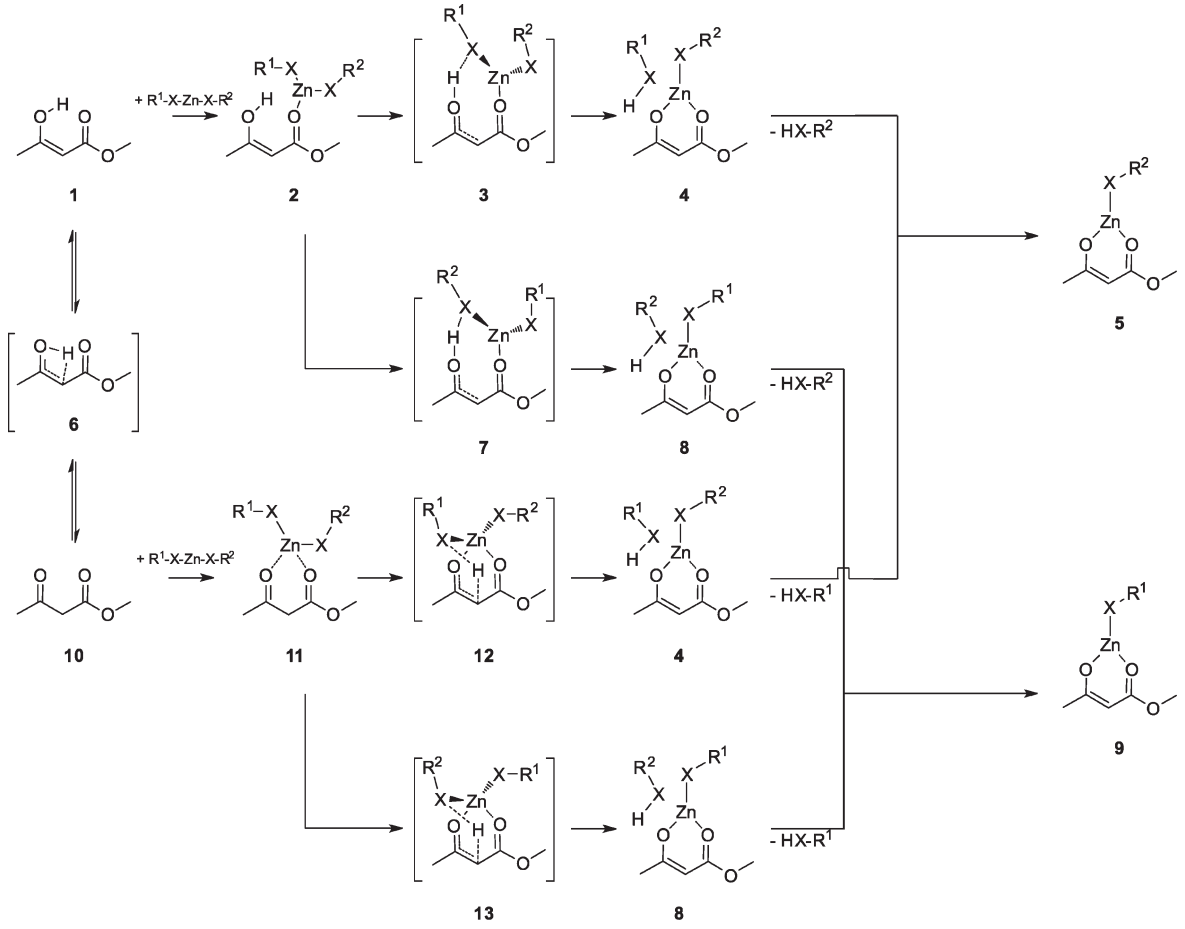

[a]X is dependent on the residues R^1 or R^2 either a carbon or an oxygen atom (see Table 1). For further calculations regarding tautomerization of **14** and **15** see the Supporting Information.

stationary points is the hybrid meta-GGA DFT functional M05-2X.[21] This functional has been optimized for nonmetal atoms and gives good results overall, especially when weak interactions are involved.[22] Despite parametrization for nonmetal atoms, it functions astonishing well for zinc-containing organometallic compounds and is therefore perfectly suited for this body of work.[23] For all atoms except iodine, the 6-311+G(2d,2p) basis set as implemented in Gaussian03 was used throughout. This basis set describes the second row atoms by the McLean−Chandler basis,[24] the basis set of McGrath and Curtiss[25] for third row atoms, and the Watchers−Hay basis set[26] for the first row of transition metals using the scaling factors of Raghavachari and Trucks.[27] As recommended when calculating transition metals, diffuse, as well as polarized, functions were used.[27] Iodine was described by a special modification of the 6-311G basis set.[28]

All stationary points were characterized with a frequency analysis, where minima must have no imaginary frequencies and the saddle points exactly one imaginary frequency. All given energies are free Gibb's energies (in kJ/mol) relative to the free and separated educts, which are zero point and thermally corrected. Therefore, all reported energetic values refer to standard conditions such as 298 K and 1 atm pressure.

All structures were previously optimized using the combination of the common hybrid DFT functional B3LYP[29] and the lanl2dz basis set, which is the combination of the D95 V[30] basis set on the first row atoms with the Los Alamos ECP plus DZ for the heavy atoms, which includes iodine.[31] Consequently, this method was used to verify all found transition states by

(21) Zhao, Y.; Schultz, N. E.; Truhlar, D. G. *J. Chem. Theory Comput.* **2006**, *2*, 364.

(22) (a) Zhao, Y.; Truhlar, D. G. *Org. Lett.* **2006**, *8*, 5753. (b) Zhao, Y.; Truhlar, D. G. *J. Phys. Chem. A* **2006**, *110*, 5121. (c) Zhao, Y.; Truhlar, D. G. *Acc. Chem. Res.* **2008**, *41*, 157.

(23) Sorkin, A.; Truhlar, D. G.; Amin, E. A. *J. Chem. Theory Comput.* **2009**, *5*, 1254.

(24) (a) Krishnan, R.; Binkley, J. S.; Seeger, R.; Pople, J. A. *J. Chem. Phys.* **1980**, *72*, 650. (b) McLean, A. D.; Chandler, G. S. *J. Chem. Phys.* **1980**, *72*, 5639.

(25) (a) Binning, R. C. J.; Curtiss, L. A. *J. Comput. Chem.* **1990**, *11*, 1206. (b) McGrath, M. P.; Radom, L. *J. Chem. Phys.* **1991**, *94*, 511. (c) Curtiss, L. A.; McGrath, M. P.; Blaudeau, J.-P.; Davis, N. E.; Binning, R. C. J.; Radom, L. *J. Chem. Phys.* **1995**, *103*, 6104.

(26) (a) Wachters, A. J. H. *J. Chem. Phys.* **1970**, *52*, 1033. (b) Hay, P. J. *J. Chem. Phys.* **1977**, *66*, 4377.

(27) Raghavachari, K.; Trucks, G. W. *J. Chem. Phys.* **1989**, *91*, 1062.

(28) (a) Glukhovtsev, M. N.; Pross, A.; McGrath, M. P.; Radom, L. *J. Chem. Phys.* **1995**, *103*, 1878. (b) Glukhovtsev, M. N.; Pross, A.; McGrath, M. P.; Radom, L. *J. Chem. Phys.* **1996**, *104*, 3407.

(29) (a) Becke, A. D. *Phys. Rev. A* **1988**, *38*, 3098. (b) Lee, C.; Yang, W.; Parr, R. G. *Phys. Rev. B* **1988**, *37*, 785. (c) Becke, A. D. *J. Chem. Phys.* **1993**, *98*, 5648.

(30) Dunning, T. H. J.; Hay, P. J. *Modern Theoretical Chemistry*; Plenum Press: New York, 1976; Vol. 3.

(31) (a) Hay, P. J.; Wadt, W. R. *J. Chem. Phys.* **1985**, *82*, 270. (b) Hay, P. J.; Wadt, W. R. *J. Chem. Phys.* **1985**, *82*, 299. (c) Wadt, W. R.; Hay, P. J. *J. Chem. Phys.* **1985**, *82*, 284. (d) Denmark, S. E.; Edwards, J. P.; Wilson, S. R. *J. Am. Chem. Soc.* **1991**, *113*, 723.

performing an intrinsic coordinate calculation (IRC)[32] with a subsequent optimization to the preceding and following intermediates. All optimizations were carried out with the GDIIS optimizer.[33] Solvent corrected geometries and energies were calculated with C-PCM as implemented in Gaussian03.[34] In this model, the species of interest are embedded in a cavity of molecular shape surrounded by a polarizable continuum, whose field modifies the energy and physical properties of the solute. The solvent reaction field is described by polarization charges distributed on the cavity surface. This procedure is known to reproduce experimental solvation energies quite well. We chose to use parameters for dichoromethane, since this is the solvent used in the experimental investigations.

Results and Discussion

A. Deprotonation Step. The deprotonation step is critical and must convert the β-keto ester into an enolate for subsequent insertion. It was assumed that the deprotonation is performed by the ethyl residue of the Furukawa reagent, as the production of ethane had been observed in NMR studies.[35] Although it is clear that the reaction can be driven by the production of ethane, a second possibility of enolate formation through generation of iodomethane was calculated for comparison reasons. Furthermore it is not clear how the acidic hydrogen is procured. The proton could be abstracted from either the enol (**1**, see Scheme 2) or the keto (**10**) structure. This is important, as both structures are in equilibrium and depending on what mechanism is favored, the facility of the tautomerization could have an impact on the overall reaction rate. Thus, both deprotonation reaction mechanisms were calculated (see Scheme 2 and Table 1).

In general, zinc enolates prefer, in the absence of significant steric hindrance, to allow the zinc ion to be complexed by two oxygen atoms. In the case of monocarbonyl enolates this will lead to the formation of dimeric structures, where one oxygen atom is coordinated by two zinc organyls, which are bearing two residues often bridged by a second, nonsymmetrical enolate.[36] As the β-keto motif provides two oxygen atoms for complexation, it is not necessarily clear whether complexed dimers would form.

Several reactions are reported[12] in which the Furukawa reagent was unable to efficiently deprotonate the β-keto ester, therefore preventing formation, or at best giving low yields, of the chain extension reaction. This is often a result of the low acidity of the α-hydrogens, for example, due to steric factors.[6] In those cases, either adding the diethylzinc first to effect deprotonation followed by addition of diiodomethane to build the Furukawa reagent,[35] or using the Xue[37] modified reagent ($CF_3CO_2ZnCH_2I$) can lead to increased reactivity.

TABLE 1. Gibb's Free Energies Relative to the Separated Educts Related to Scheme 2

	diethylzinc	Furukawa	Xue
	R^1-X = R^2-X = ethyl	R^1-X = ethyl; R^2-X = CH_2I	R^1-X = CF_3CO_2; R^2-X = CH_2I
1	0	0	0
2	18	11	−40
3	65	63	6
4	−134	−132	−34
5	−134	−159	−159
6	257	257	257
7	−[a]	67	46
8		−114	−150
9		−134	−157
10	13	13	13
11	33	2	−58
12	82	77	18
13		88	59

[a]These values are not available, as both residues R^1 and R^2 are equal (see Scheme 2).

Consequently, energetics of initial deprotonation steps utilizing either diethylzinc, the Furukawa reagent, or $CF_3CO_2^-$ $ZnCH_2I$ were calculated based on reaction with either the enol (**1**) or the keto (**10**) structure (cf. Scheme 2 and Table 1).

The energy values of the transition states **3** (63 kJ/mol), **7** (67 kJ/mol), **12** (77 kJ/mol), and **13** (88 kJ/mol) in the case of the Furukawa reagent show that there is no substantial kinetic preference, which could explain the favored formation of ethane, as they differ only by ∼10 kJ/mol. Production of ethane (**4**; −132 kJ/mol) is more exothermic than formation of iodomethane (**8**; −114 kJ/mol), but this thermodynamic preference disappears upon dissociation of the ethane and iodomethane byproducts, in that pure products **5** and **9** (i.e., not in interaction with any byproducts) possess nearly the same energies.

In the case of the Xue reagent the calculations predict a kinetic preference for deprotonation with the CF_3COO^- moiety, as opposed to the iodomethyl group. The transition state for deprotonation with the CF_3COO^- group is preferred either by 40 kJ/mol in case of the enol (**3**) or 31 kJ/mol with the ketone (**12**).

The deprotonation potential of diethylzinc in comparison to the Furukawa reagent is higher, both experimentally[12] and by probability, due to the presence of one more ethyl residue in comparison to the Furukawa reagent. However, the activation barriers, as well as the products, possess nearly the same energies in the case of diethylzinc or the Furukawa reagent.

Since the deprotonation reaction involving the enol form and the keto form both appear kinetically viable, the rate of tautomerization would not be expected to play a significant role in the deprotonation reaction.[38]

The main difference in energy between the enolate and the keto transition states is due to steric effects (see Figure 1). While the transition state generated from the enol form involves a four-membered ring (**3** and **7**), the transition state resulting from the ketone resembles a favored six-membered ring (**12** and **13**); however, this forces the zinc ion to a less than optimal position relative to the coordinating oxygen atoms, which lowers the coordination energy significantly,

(32) (a) Fukui, K. *Acc. Chem. Res.* **1981**, *14*, 363. (b) Hratchian, H. P.; Schlegel, H. B. *Theory and Applications of Computational Chemistry: The First 40 Years*; Elsevier: Amsterdam, The Netherlands, 2005.

(33) (a) Pulay, P. *Chem. Phys. Lett.* **1980**, *73*, 393. (b) Pulay, P. *J. Comput. Chem.* **1982**, *3*, 556. (c) Császár, P.; Pulay, P. *J. Mol. Struct.* **1984**, *114*, 31. (d) Farkas, O.; Schlegel, H. B. *J. Chem. Phys.* **1999**, *111*, 10806.

(34) (a) Klamt, A.; Schüürmann, G. *J. Chem. Soc., Perkin Trans. 2* **1993**, 799. (b) Barone, V.; Cossi, M. *J. Phys. Chem. A* **1998**, *102*, 1995. (c) Cossi, M.; Rega, N.; Scalmani, G.; Barone, V. *J. Comput. Chem.* **2003**, *24*, 669.

(35) Hilgenkamp, R.; Zercher, C. K. *Org. Lett.* **2001**, *3*, 3037.

(36) (a) Hansen, M. M.; Bartlett, P. A.; Heathcock, C. H. *Organometallics* **1987**, *6*, 2069. (b) Hlavinka, M. L.; Hagadorn, J. R. *Organometallics* **2006**, *25*, 3501.

(37) (a) Xue, S.; Li, L.-Z.; Liu, Y.-K.; Guo, Q.-X. *J. Org. Chem.* **2005**, *71*, 215. (b) Xue, S.; Liu, Y.-K.; Li, L.-Z.; Guo, Q.-X. *J. Org. Chem.* **2005**, *70*, 8245.

(38) Sonnenberg, J. L.; Wong, K. F.; Voth, G. A.; Schlegel, H. B. *J. Chem. Theory Comput.* **2009**, *5*, 949.

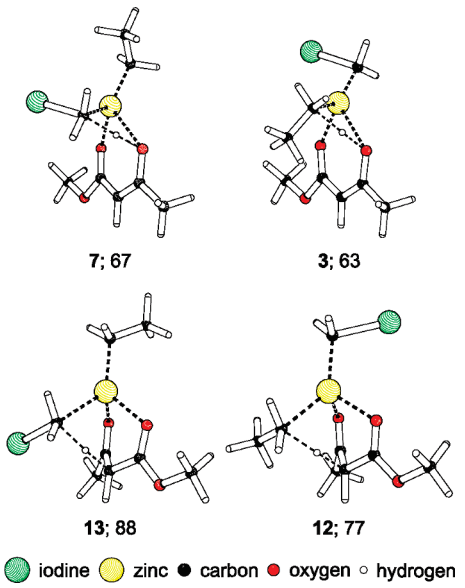

FIGURE 1. Structures of several deprotonation transition states involving the Furukawa reagent.

forcing the carbon frame to contort, and thus creating a significant increase in energy.

NBO calculations show that the bonding arrangement in **5** is exactly as depicted in Scheme 2. Although a delocalized electron distribution is conceivable, the bond order of the carboxylate carbon−oxygen double bond, as well as the depicted carbon−carbon double bond, is exactly two. This means that enolate formation and zinc complexation fixes the carbon−carbon double bond and enhances the electron density at this coordinate, hence electrophilic attack at this bond is easily facilitated.

B. Carbenoid Insertion. The carbenoid insertion step in the traditional Simmons−Smith reaction follows two mechanistic pathways. The first is a concerted insertion of the methylene moiety into the double bond with concomitant formation of an iodine−zinc bond (methylene transfer), and the second is a two-step carbometalation mechanism, i.e. addition of methylene and the metal center to the double bond, followed by carbon−carbon bond formation and loss of the metal.[17j]

In contrast to the structural situation of the traditional Simmons−Smith reaction, the substance on which the carbenoid insertion step is performed during the chain extension reaction is a zinc enolate. Additionally, a second oxygen atom present in the starting material's ester functionality offers opportunity for additional complexation. Since oxygen is known to complex strongly to zinc ions, precoordination effects are expected.

As depicted in Scheme 3, the mechanistic pathway begins at intermediate **16** (identical to structure **5** of the deprotonation pathway with the Furukawa reagent, see Scheme 2) or encounter complex **17**, respectively. As the zinc ion is bearing an iodomethyl ligand, an intramolecular carbenoid insertion step is conceivable (path C). On the other hand, a second Furukawa reagent could approach and attack the carbon−carbon double bond (paths A and B). This requirement for 2 equiv of carbenoid is not an unreasonable situation, as the carbenoid is usually administered in excess.

In contrast to the Simmons−Smith reaction a carbometalation transition step could not be found in any of the mechanistic pathways (A, B, and C). This is most likely due to the existence of oxygen atoms in close proximity to the carbon−carbon double bond, which easily coordinate the zinc atom of the approaching Furukawa reagent (Figure 2, structure **20**). In the case of the transition state (**18**) resulting from intramolecular delivery of the carbenoid, the zinc ion is already coordinated by oxygen atoms, thereby making carbometalation involving this zinc atom less likely.[17j] Therefore, in all three cases a methylene transfer transition state can be envisaged leading to formation of a carbon−carbon bond between the carbenoid and the central carbon atom within the double bond (see Scheme 3, structures **18**, **20**, and **22**).

SCHEME 3. Three Possible Pathways of the Methylene Insertion Step[a]

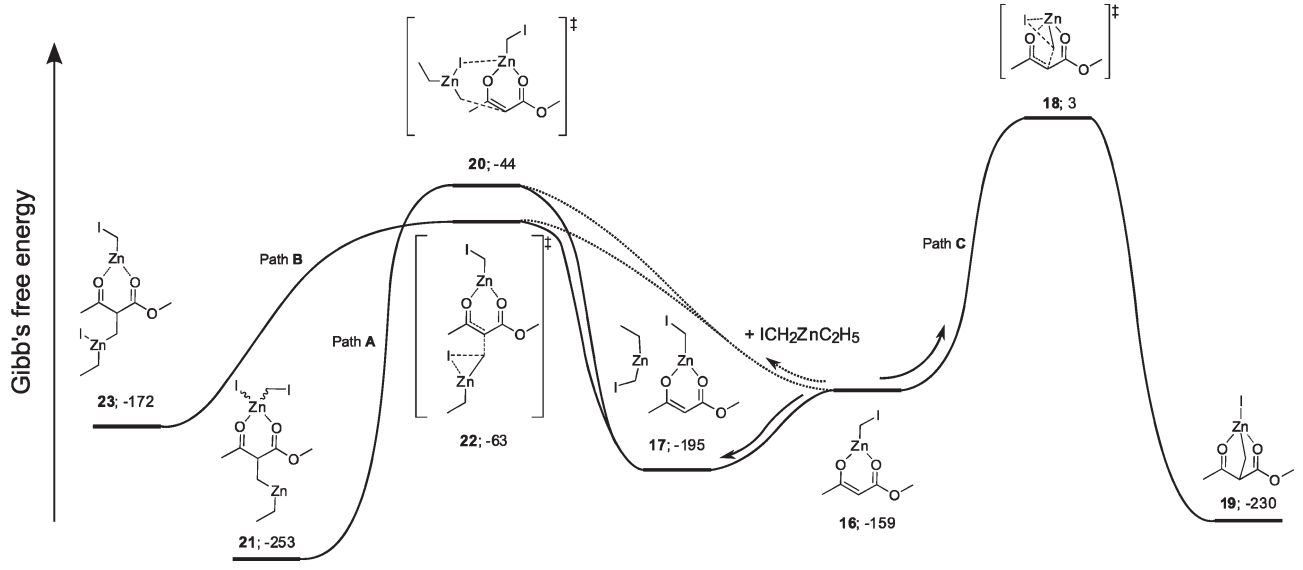

[a]The curves are not representing any functional correlation but are only implemented to better fit the Lewis formulas.

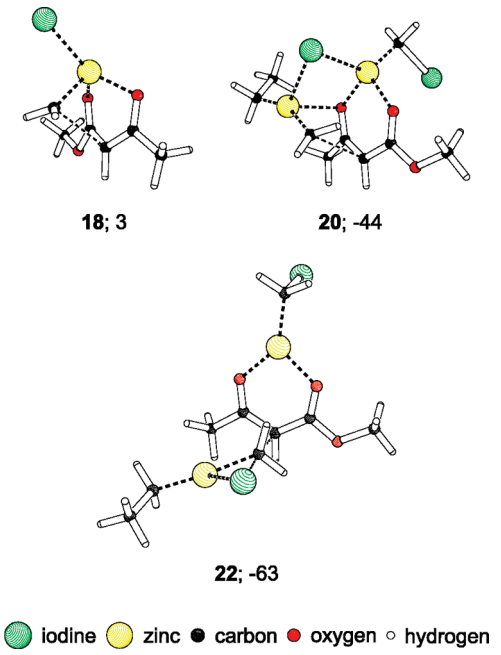

FIGURE 2. Structures of several carbenoid insertion transition states.

SCHEME 4. Pathway C: The Intramolecular Methylene Insertion

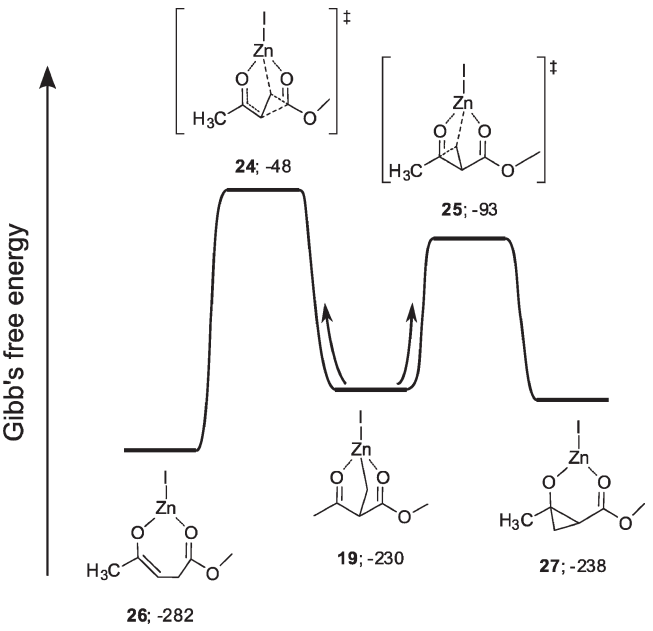

This carbon atom is clearly the most negatively charged in the diketo structure (**10**) (also verified by NBO calculations), and the carbon−carbon bond is formed in a concerted fashion with the formation of an iodine−zinc bond. To our surprise, however, all transition states (**18**, **20**, and **22**) did not lead directly to the classical cyclopropane intermediate, as is known for the Simmons−Smith reaction. Instead a zinc homoenolate intermediate, in which the carbenoid is bound to one carbon atom of the former carbon−carbon double bond and to the zinc atom, is favored.

Although the three transition states have similar mechanistic characteristics, they differ slightly. The transition state (**18**, path C) arising from intramolecular delivery of the carbenoid is the most similar to the Simmons−Smith methylene transfer mechanism. This leads to a very tightly closed ring intermediate with an activation barrier 47 kJ/mol higher than that of **20** and 66 kJ/mol higher than that of **22** (see Figure 2), which suggests that the probability of pathway C is rather low. Pathways A and B proceed from the encounter complex **17**, which is 26 kJ/mol more stable than intermediate **16**. As it is not clear whether this structure (**17**) will be in existence in solution, pathways A and B could also proceed directly from **16** (dotted lines). This would further reduce the activation energies in comparison to pathway C.

In comparison to **18**, transition structure **20** from pathway A has a more relaxed conformation (see Figure 2) as a second Furukawa reagent attacks the carbon−carbon double bond. In contrast to the Simmons−Smith reaction, the iodine atom of the Furukawa reagent is not transferred to the zinc ion of the attacking substrate, but to the zinc atom complexed to the oxygens.

An alternative path from **17** (path B) is kinetically favored, as it contains the lowest transition state (**22**). In this structure the complexation variability of the zinc metal becomes apparent. Whereas in all previous structures the zinc atom established exactly two covalent bonds to organic residues (besides some complexation bonds), the zinc atom of the former attacking Furukawa reagent bears three residues in intermediate **23**, while the former zinc enolate moiety only has one covalent bond, explaining the higher energy of this intermediate compared to the other two pathways.

Pathway C. Although path C is kinetically compromised, it was investigated further for completeness. After the formation of the intramolecular bridged structure **19**, two transition states leading to chain extension are conceivable. The carbon atom of the former carbenoid could attack at the atom of either the carboxylate (**24**, see Scheme 4) or keto (**25**) moieties.

Dependent on which carbon atom has been attacked, either a cyclopropane intermediate (**27**) or a direct chain homologation product can be envisaged (**26**), since both products are thermodynamically very stable. In comparison, the selectivity of the transition states is obvious, as the attack of the former carbenoid on the carbon atom of the keto group is much more favored due to a lower electron density of the ester residue. Experimentally, the regiospecific incorporation of the new methylene is inconsistent with the path leading through **24** to form **26**, which lends support to the computational model.

Pathway A. Considering the diketo structure **21** (see the upper graph in Scheme 5) can potentially undergo rotation at the ester residue, generating **29** in which the alkoxy functionality of the ester residue is coordinated to the zinc atom instead of the carbonyl oxygen, these alternate pathways were calculated in an effort to investigate the energetic impact of the various complexation modes (pathways a and b).

Additionally, it is conceivable to consider conversion of the homoenolate (**21**) to the chain extended material (**31** or **42**) in the absence of a coordinated zinc atom (see the lower graph in Scheme 5), as it may not be absolutely necessary to maintain the complexed structure after the alkylation of the enolate is completed. Thus those conceivable pathways were investigated computationally in order to more completely understand the entire mechanism (paths c and d).

SCHEME 5. Pathway A: In the Upper Scheme the Reaction Paths a and b Are Depicted, Which Differ by an Additional Zinc Residue Coordinated to Both Keto Oxygen Atoms As Depicted in Paths c and d (Lower Scheme)

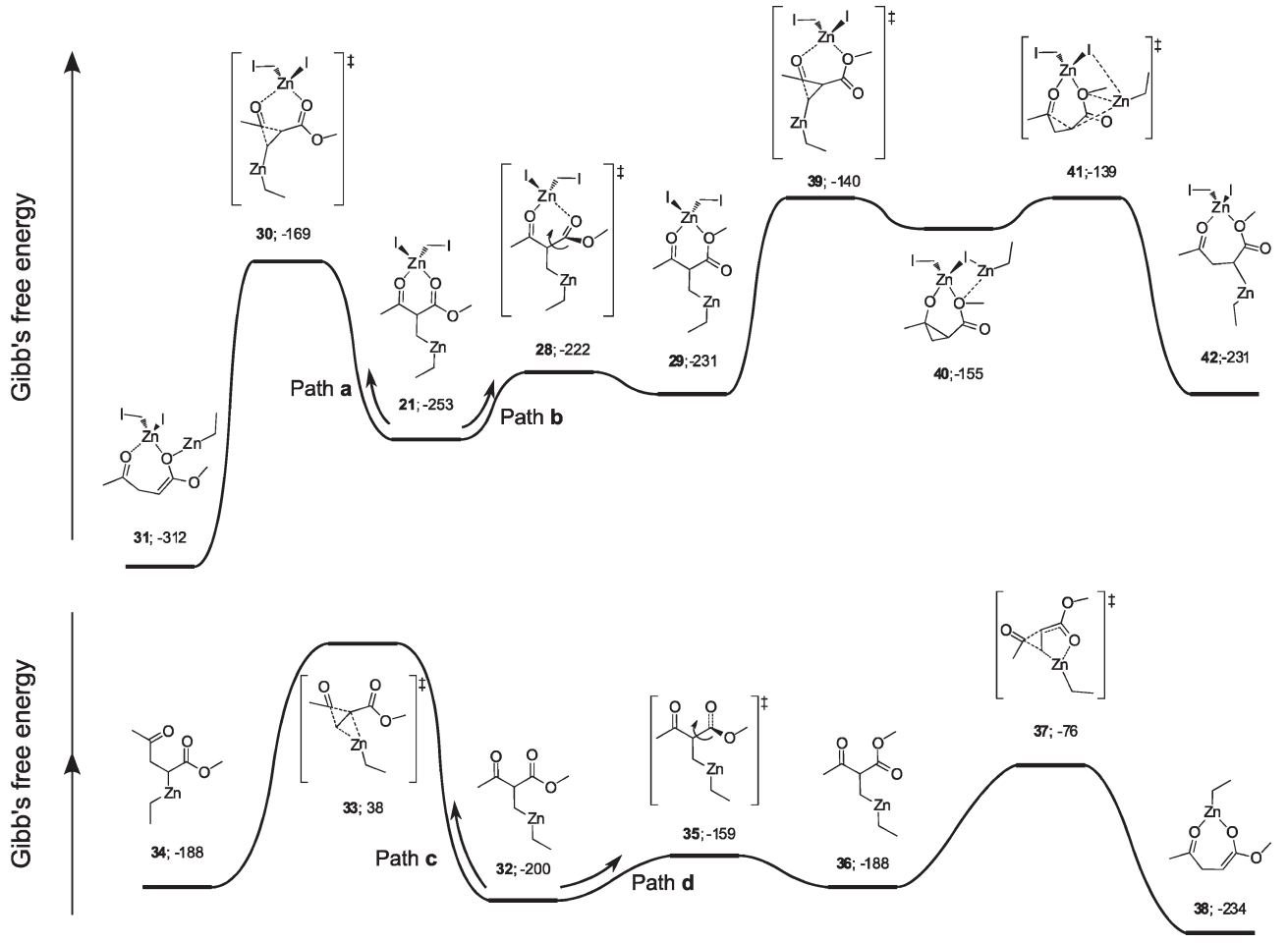

As depicted in Scheme 5, the transition state (**28**) involving rotation, leading from intermediate **21** to **29**, has a low activation barrier of 31 kJ/mol and is therefore easily surmountable. Intermediate **29** is slightly more unstable than its corresponding isomer **21**. The difference in energy, about 22 kJ/mol, is a result of the weaker interaction of the OR oxygen with the zinc atom.

Furthermore, the corresponding, uncomplexed structures **32** and **36** are also interchangeable via the rotation transition state **35**. While this activation barrier is again not high, a comparison of the intermediate's energies demonstrates that the pathway with uncomplexed intermediates is not favored. When transition states **37** and **39** are compared, it becomes even more obvious that complexation plays an important role. The two transition state structures show the attack of the former carbenoid carbon atom on either the carbon atom of the ester or the keto group such as seen in path C (see Schemes 4 and 5). While the intramolecular attack on the keto functionality from conformation **32** appears to involve concerted formation of the chain extended product together with zinc−carbon bond formation (**33**), the attack on the ketone with zinc complexation to the ester functionality results in direct formation of a chain-extended zinc enolate (**38**). The stronger zinc oxygen interaction explains the significant difference in energy between those structures **33** and **37** (114 kJ/mol). Nevertheless, when considering that both transition states (**33** and **37**) are very high in energy and that excess zinc is typically present in the reaction mixture, those pathways are very unlikely. In further support of the necessity of zinc-complexation, stoichiometry studies reveal that 1 equiv of Furukawa reagent returns starting material, whereas 2 equiv provide product,[39] supporting the requirement of enolate complexation by zinc as well as the exclusion of pathway C.

The energetics of the reaction changes significantly when a coordinated zinc substrate is involved. Mechanistically, the transition structures **30** and **39** are similar to those of the uncomplexed pathways c and d, with the zinc-containing starting material (**21**) being converted directly into an enolate (**31**) or a stepwise formation and fragmentation of a donor−acceptor cyclopropane (**40**) via transition states **39** and **41**. The increased stability of paths a and b, as compared to paths c and d, predominately derives from the zinc oxygen interactions, which lowers the activation barriers significantly. In addition, thermodynamic stability of the products improves in a significant manner. When comparing paths a and b, path a is the most preferable pathway, as it is kinetically favored (**30** is 29 kJ/mol lower than **39**). In addition, a thermodynamic driving force appears to be present, in that **31** is 81 kJ/mol more stable than **42**.

(39) Hilgenkamp, R. MS thesis.

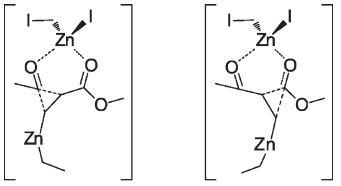

FIGURE 3. Comparison of the insertion transition state **30** and its alternative **30-c**.

An alternative cyclization pathway, involving intramolecular attack on the ester functionality, was explored through the computational modeling of **30-c**, which is 48 kJ/mol higher in energy than **30** and, therefore, deemed unlikely.

These results suggest that the pathways in which a zinc residue is complexed to the keto ester are significantly favored and that those pathways that involve a rotating ester functionality are unlikely; hence, they were not further investigated for subsequent pathways (i.e., B).

Pathway B. This pathway was predicated on the proposed classic donor−acceptor mechanism. As mentioned above, the initial alkylation event (Scheme 3) can proceed via two distinct pathways in which formation of **23** is slightly kinetically preferred (transition state **22** is 19 kJ/mol lower than **20**, see Scheme 3) but significantly disfavored thermodynamically (**23** is 81 kJ/mol less stable than **21**). These conflicting energetics require that both pathways (A and B) be fully investigated.

In analogy to pathways A (**30**, see Scheme 5) and C (**25**, see Scheme 4), mechanism B also requires a second transition state (**43**) to form the second carbon−carbon bond. This energy barrier is easily surmountable. In contrast to reaction path A, this pathway (B) contains an intermediate donor−acceptor cyclopropane (**44** and **45**, similar to pathway C), which is thermodynamically disfavored compared to its correspondent structure in path A (**31**, see Scheme 5). Surprisingly, the cyclopropane ring-opening transition state (**46**) has a very low activation barrier, but the product lacks the thermodynamic stability of the products observed in path A. Beyond intermediate **47**, the pathway could follow either an intramolecular mechanism, in which the coordinated zinc atom attacks the double bond, or a reaction with a third Furukawa reagent. Both pathways lead in principle to the same product.

Furthermore, this route requires one more reaction step to lead to the product (**50**−**52**), but neither appear to possess high energy barriers. Thus pathway B is kinetically preferred over pathway A by about 87 kJ/mol, but thermodynamically disfavored. Therefore, pathway B is, as long as the introduced amount of energy is too low to support pathway A, the preferred pathway. Otherwise, both pathways could by viable.

Similar to the pathways A and C (see Figure 3 and Scheme 4), a second insertion step **43-c** (see Figure 4) involving attack on the ester functionality is conceivable, but also not favored, as its activation barrier is 42 kJ/mol higher than that of **43**. Therefore, an insertion into the carbon−carbon bond between the methylene bridge and the keto group as in pathway B is strongly preferred.

Solvent Corrections. Solvent effects were investigated for the deprotonation step and the methylene insertion step.

In the case of the deprotonation reaction, the change in structural parameters is very small and thus the energies

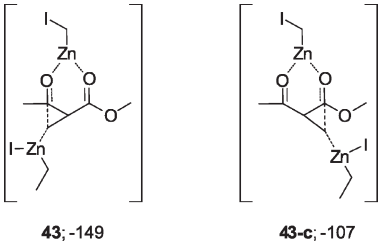

FIGURE 4. Insertion transition state **43** and its alternative **43-c**.

TABLE 2. Gibb's Free Energies and Activation Barriers Related to the Last Intermediate of Solvent and Gas Phase Optimized Geometries

	gas phase		solvent corrected	
	ΔG	$\Delta\Delta G_a$	ΔG	$\Delta\Delta G_a$
1	0		0	
2	11		7	
3	63	63	62	62
4	−132		−111	
5 (**16**)	−159		−188	
18	3	162	−72	116
20	−44	115	−60	128
21	−253		−272	
30	−169	84	−238	34
22	−63	96	−152	36
23	−172		−273	
43	−149	23	−234	39

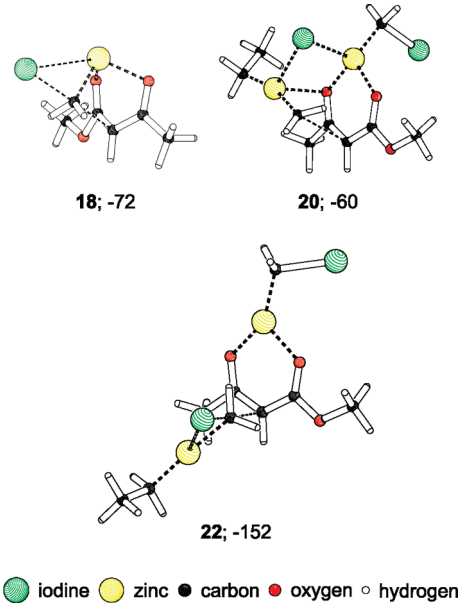

FIGURE 5. Solvent corrected structures of the insertion transition states depicted in Figure 2.

do not change significantly. The reaction becomes more exothermic without losing its kinetic preference. In the case of the three possible insertion reaction transition states a change is obvious, as the free energies relative to the educts (ΔG) and the activation barriers relative to **5** ($\Delta\Delta G_a$) are different in comparison to the gas phase energies (Table 2). While transition state **20**, which introduces pathway A and leads to a mechanism without a cyclopropane intermediate, does not experience a large change in energy, the activation barrier of **22**, which leads to pathway B, and **18** drops vastly. An explanation for this behavior is illustrated in Figure 5.

SCHEME 6. Pathway B

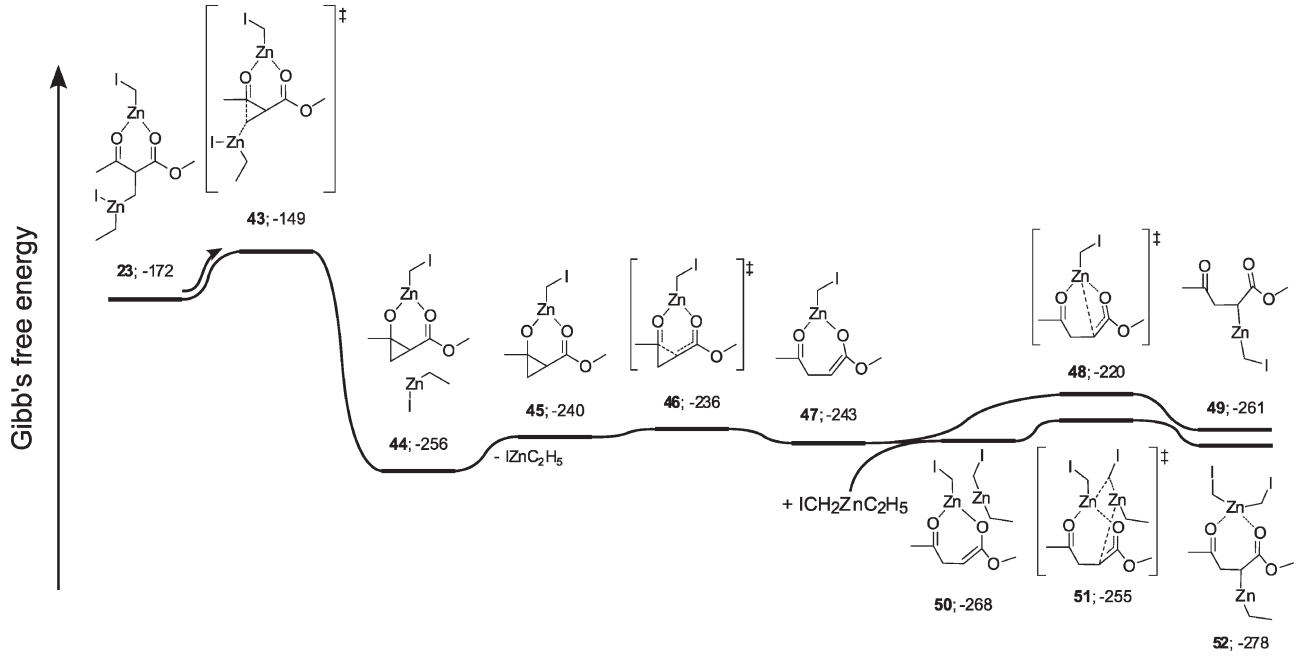

When compared to the gas phase structures in Figure 2, the geometries of **18** and **22** are changed significantly, with the primary changes occurring at the zinc and iodine portion of the molecules. These structures are able to relax their geometries as a result of the solvent influence. In the case of transition state **20**, the coordination of the Furukawa reagent via the zinc and the oxygen atom is so rigid that solvent-induced relaxation of the geometry is not apparent. Therefore, the geometry is not affected by the forces introduced by the solvent and the energy of the transition state does not drop. An alternative explanation is the influence of the solvent regarding the charge distribution in the molecule. As pathway B includes triple valence zinc atoms, an increase of electron density on this atom is reasonable. A NBO analysis shows that even if the solvent is not able to influence the difference in charge between the double and triple valence zinc atom, it shifts the electron density to significantly lower values and therefore lowers the energy of the whole system (see the Supporting Information).

As a result, the solvent-corrected calculations support the incorporation of the methylene group via pathway B and thus a mechanism that includes a cyclopropane intermediate, even if the cyclopropane possesses only a short lifetime.

Dimers. The reactive intermediate formed in the Reformatsky reaction, generated by zinc insertion into the carbon−halogen bond of a α-haloester, is dimeric in nature. X-ray crystallography and ebulliometry in THF has shown that the intermediate is a carbon-bound zinc organometallic structure, and that it is a dimer in both solution and in solid state.[40] Observations made by ^{1}H and ^{13}C NMR spectroscopy in a variety of coordinating solvents[16b] have also shown the Reformatsky intermediate to possess a carbon-bound zinc. Preliminary NMR investigations by Zercher[16a] suggest the existence of a zinc−carbon bond in the homologation reaction studied herein, therefore pathway A or B (Schemes 5 and 6) could potentially be differentiated by calculating dimeric structures using intermediates **31**, **49**, or **52**. In this view three dimeric structures (**D-1**, **D-2**, and **D-3**) were calculated (see Scheme 7).

SCHEME 7. Calculated Dimeric Structures As Mixtures of 31 (Pathway A) and 52 (Pathway B)

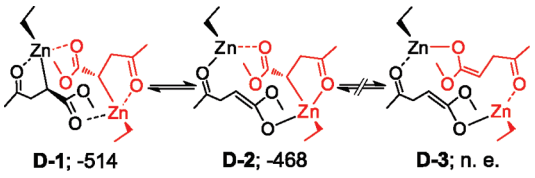

D-1, which is a pure dimer of **52**, is more stable than **D-2**. **D-2** consists of **52** and **31**, whereas the nonstable geometry **D-3** is a pure dimer of intermediate **31**. These calculations show that even if the equilibrium before quenching is reached by pathway A, a zinc−carbon bond can be present. Therefore the existence of this bond does not exclude this mechanism (pathway A). On the other hand, these calculations provide further support for pathway B, because **D-1**, the dimeric structure of **52**, is now thermodynamically favored.

Conclusion

Computational results suggest that the rate determining step of the zinc carbenoid-mediated chain extension reaction is the deprotonation step. While proton abstraction is easier from the enol tautomer, deprotonation of both the enol and the keto tautomers is reasonable and the reaction is not dependent on the tautomerization transition state. Furthermore, the deprotonation step is clearly the rate determining step, as it has the highest activation barrier. The deprotonation step is facile, as both the reactions with the ethyl or the diiodomethyl residues have reasonable activation barriers. However, ethane has been observed by NMR suggesting it

(40) Dekker, J.; Boersma, J.; van der Kerk, G. J. M. *J. Chem. Soc., Chem. Commun.* **1983**, 553.

is the dominate base. Contrarily, the reaction with Xue's reagent is clearly energetically favored, what is mostly an effect of the more electronegative oxygen (compared to carbon). As this is kinetically favored, it can enhance the reaction rate even at low temperatures. The use of only diethylzinc first to deprotonate and diiodomethane later to build the carbenoid seems to be a result of two ethyl residues.

As described above, three possible mechanisms of carbenoid insertion have been proposed. The presence of oxygen atoms in the proximity of the zinc carbenoid results in different transition states compared to the traditional Simmons−Smith reaction. Carbometalation transition states are not only disabled by the oxygen complexation, but the oxygens also appear to stabilize resulting intermediates, which promotes a two-step mechanism. While the intramolecular insertion of the carbenoid carbon via pathway C is disfavored, a preference for pathway A or B is not clear. Pathway A (a) is thermodynamically favored and needs only two transition states to reach the stable intermediate. Alternatively, the activation barriers of the insertion steps in pathway B are lower, but it involves a cyclopropane intermediate that requires an additional transition state. Therefore, both reaction pathways are considered reasonable. An investigation of transition state energies that involve solvent correction suggests pathway B to be the most favorable pathway.

The computational results explain the absence of a cyclopropane intermediate in preliminary NMR studies. Although pathway B proceeds via such an intermediate, the subsequent transition state has such a low activation barrier that it does not support a significant half-life for a cyclopropane intermediate. In contrast to the traditional donor−acceptor intermediate predicted in pathway B, this body of work unveiled a surprising alternative mechanism (A), which does not include the donor−acceptor cyclopropane intermediate, but has a cyclopropane transition state also supporting the NMR results.

Lastly, this study has concentrated on monomeric species only, even though dimeric species are conceivable. A more complete understanding of the involvement of dimeric species will require the involvement of additional spectroscopic analyses. This is currently under investigation and will be reported in due course.

Acknowledgment. Computational resources used in this work were provided by the University of Queensland (Centre for Computational Molecular Science) and the Australian Research Council (LIEF grant LE0882357: A Computational Facility for Multiscale Modelling in Computational Bio and Nanotechnology).

Supporting Information Available: Cartesian coordinates as well as total and relative energies at each level of theory for the optimized stationary points. This material is available free of charge via the Internet at http://pubs.acs.org.